



Long-distance neural synchrony correlates with processing strategies to compare fractions



Paulo Barraza*, David M. Gómez, Felipe Oyarzún, Pablo Dartnell

Centro de Investigación Avanzada en Educación, CIAE, Universidad de Chile, 8330014 Santiago, Chile

HIGHLIGHTS

- Long-distance neural synchrony modulated by fraction processing strategies.
- Alpha phase desynchronization induced by componential processing strategy.
- Theta and Gamma phase synchronization induced by holistic processing strategy.
- Holistic processing strategy evoked right anterior negativity around 400 ms.
- Early theta phase synchrony correlate with anterior negativity around 400 ms.

ARTICLE INFO

Article history:

Received 30 November 2013

Received in revised form 5 March 2014

Accepted 17 March 2014

Keywords:

Neuronal synchrony

EEG

Fraction processing

Theta band

Alpha band

Gamma band

ABSTRACT

Adults use different processing strategies to work with fractions. Depending on task requirements, they may analyze the fraction components separately (componential processing strategy, CPS) or consider the fraction as a whole (holistic processing strategy, HPS). It is so far unknown what is the brain coordination dynamics underlying these types of fraction processing strategies. To elucidate this issue, we analyzed oscillatory brain activity during a fraction comparison task, presenting pairs of fractions either with or without common components. Results show that CPS induces a left frontal-parietal alpha phase desynchronization after the onset of fraction pairs, while HPS induces an increase of phase synchrony on theta and gamma bands, over frontal and central-parietal sites, respectively. Additionally, the HPS evokes more negative ERPs around 400 ms over the right frontal scalp than the CPS. This ERP activity correlates with the increase of Theta phase synchrony. Our results reveal the emergence of different functional neural networks depending on the kind of cognitive strategy used for processing fractions.

© 2014 The Authors. Published by Elsevier Ireland Ltd. This is an open access article under the CC BY license (<http://creativecommons.org/licenses/by/3.0/>).

1. Introduction

Recent research has demonstrated that educated adults use different strategies to solve problems involving fractions: in some contexts, adults consider only the fractions' numerators and denominators [1], whereas in other contexts they give signs of accessing the fractions' numerical magnitudes [2]. The adult brain seems to select between strategies based on isolated fraction components (componential processing strategies, CPS) and strategies based on the numerical fraction magnitude (holistic processing

strategies, HPS) depending on task demands [1]. In the case of fraction comparison, the CPS is favored when the fractions to be compared share a common component (e.g., $1/4$ vs. $1/9$ or $2/6$ vs. $3/6$) [1], whereas the HPS is preferred when the fractions lack common components (e.g., $5/9$ vs. $6/8$ or $3/6$ vs. $2/5$) [2].

To date, few studies have investigated the brain correlates of these processing strategies. A recent ERP study [3] showed that the use of the CPS while comparing fractions of the form $1/n$ to the standard $1/5$ elicits a P3 component, whose latency grows if the stimulus set to compare to $1/5$ comprises both fractions and decimals (e.g., $1/3$, 0.2). This mixed condition also evoked an N2 component over frontal electrodes, probably reflecting higher cognitive demands [3]. In addition, a functional magnetic resonance study [4] has investigated the brain areas involved in fraction comparison and found that whereas both the CPS and the HPS activate frontoparietal regions, only the HPS modulates activity in the intraparietal sulcus, a region traditionally associated with the mental representation of numerical magnitude [5].

* Corresponding author at: Centro de Investigación Avanzada en Educación, Periodista José Carrasco Tapia 75, 8330014 Santiago, Chile. Tel.: +56 2 29770911; fax: +56 2 2978 2762.

E-mail addresses: paulo.barraza@ciae.uchile.cl (P. Barraza), dgomez@ciae.uchile.cl (D.M. Gómez), felipe.oyarzun@ciae.uchile.cl (F. Oyarzún), dartnell@dim.uchile.cl (P. Dartnell).

Although ERPs provide fine-grained information about the time course of fraction processing strategies and the fMRI data indicate what are the relevant brain structures associated to these processes, the oscillatory dynamics of the neural networks involved may provide us with additional valuable information about the mechanisms underlying the processing of fractions. In this article, we analyze local and long-distance neuronal synchrony activity [6], which are well-established ways to investigate the dynamics of functional network formation during cognitive information processing [7–9]. There are many ways of quantifying neural synchrony. Here we focus on two of them: The first one is induced spectral power analysis, or amplitude variations in EEG oscillatory activity [10]. This measure is a good indicator of synchronization of large groups of neurons located in the same brain region [11]. The second analysis measures phase coupling, that is to say the relative stability of the difference of phases between pairs of electrodes [6]. High values of phase coupling between two electrodes suggest that large groups of neurons far from each other are functionally related [6]. Thus, induced spectral power and phase synchrony provide us with two measures containing different, but complementary, information.

In the present study we explore the local and long-distance neural synchronization correlates of the CPS and the HPS in the processing of fractions. Additionally, we analyze ERPs for comparison with previous results [3]. We recorded EEG signals in subjects engaged in a fraction comparison task. To elicit preferentially either the CPS or the HPS, we presented pairs of fractions with and without common components, respectively [4]. As indicators of local and long-distance neural coordination, we measured over a wide frequency range the induced spectral power of local signals [10] and the phase synchronization across recording sites [6,12]. We found that CPS and HPS differ with respect to global synchronization and ERP, but not to local neural processing. We propose that long-distance neural integration is the critical event that mediates the efficient allocation of cognitive resources during processing of fractions.

2. Methods

2.1. Subjects

Twenty subjects (11 males, age range: 18–41 years, mean age = 28.4 years) participated in an EEG experiment. Five subjects were excluded from the analysis because they presented less than 50 percent of artifact-free EEG trials per experimental condition (total trials per condition = 78; mean artifact-free trials: CPS = 67.9, HPS = 62.4). All participants were native Spanish speakers, right handed, with normal hearing and normal or corrected to normal vision, and with no history of neurological and/or psychiatric illness. The Ethical Committee of the Medicine Faculty of the University of Chile approved the protocols used in this study, and all participants gave written informed consent before being tested.

2.2. Stimuli

We used 156 different pairs of fractions with single-digit numerators and denominators in a fraction comparison task. All numerators and denominators were in the range 1–9, such that the resulting fractions were always proper. Fractions were presented as two vertically displaced digits separated by a horizontal line and displayed in silver color on a black background. Each fraction measured 1.5 cm × 5.5 cm (width × height). Fractions were located 2 cm to the left or right of the center of the screen. Viewing distance was 63 ± 3 cm.

We grouped fraction pairs into two blocks of trials to better study the CPS and HPS, as suggested previously [4]. In the CPS block, fraction pairs had a common component (either a common numerator, e.g. 1/6 and 1/8, or a common denominator, e.g. 2/7 and 4/7), whereas in the HPS block, fraction pairs had no common component (e.g. 3/7 and 2/9). Each block consisted of 78 pairs of fractions. Within each block, the order of presentation of fraction pairs was pseudo-random. The order of presentation of the two blocks was counterbalanced between subjects.

2.3. Procedure

Prior to the experiment, participants read the instructions for the fraction comparison task. Each experimental trial began with the presentation of a fixation cross in the center of the screen (duration between 1500 and 2400 ms), followed by the visual presentation of the fraction pair (3000 ms), and finally by a question mark that appeared on the screen as a cue for subjects to respond. In this period, subjects indicated which one of the two fractions was the largest by pressing one of two possible response buttons. The question mark remained on the screen until the subject pressed a button.

EEG recording was performed inside a Faraday cage. The fraction comparison task was programmed with the stimulus presentation software E-Prime version 2.0. The pairs of fractions were presented visually in the center of a PC monitor screen and behavioral responses were collected with a response pad EGI 200.

2.4. Data analysis

EEG activity was recorded with 64-sensor HydroCel GSN nets referenced to vertex (Electrical geodesics, Eugene, OR, USA). The EEG was filtered online from 0.01 to 100 Hz in order to eliminate DC fluctuations, and digitized at 1000 Hz. Electrode impedances were below 40 k Ω , the optimal level for this system [13]. Finally, the signal was stored for offline analysis.

2.4.1. Induced spectral power and phase synchrony

The raw EEG signal was first segmented into a series of epochs lasting 3400 ms including 1200 ms preceding the onset of the fraction pair, and then re-referenced off-line to average reference. Electrodes placed near the eyes and face were excluded from analysis. Thus, we estimated phase synchrony for 59 out of 64 channels. The continuous 50 Hz (AC) components were filtered in each epoch with a zero-phase filter that keeps the biological 50 Hz signal. Trials containing voltage fluctuations that exceeded $\pm 200 \mu\text{V}$ or transients exceeding $\pm 100 \mu\text{V}$ were excluded from analysis.

The artifact-free signal was then processed with a sliding-window fast Fourier transform (window length, 256 ms; step, 10 ms). By this process we obtained amplitude and phase values for frequencies between 1 and 90 Hz with 1 Hz frequency resolution. Then, amplitude information was used to compute the induced spectral power that is obtained by averaging the time-frequency energy across single trials (see [10] for details), while the phase information was used to obtain the phase-locking value (PLV) [12]. In brief, this method involves computing the phase difference in a time window for each electrode pair and assessing the stability of such phase difference through all trials and all different frequencies in the EEG.

The charts of induced spectral power and phase synchronization were normalized to a baseline period starting 400 ms before the onset of the fraction pair. We normalized the signal by subtracting the average activity of the baseline from the raw signal and then dividing by the standard deviation of the baseline, in a frequency-by-frequency manner.

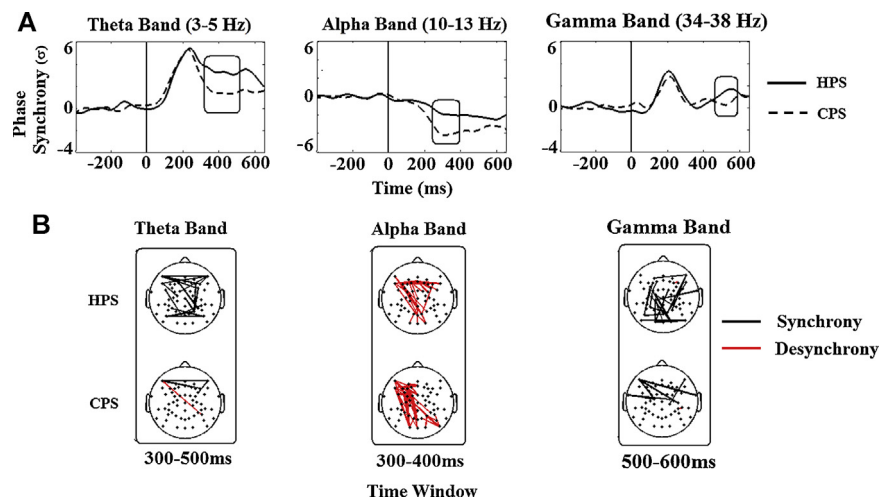


Fig. 1. Phase synchrony and its scalp distribution during the processing and comparison of fractions. (A) Contrasts between conditions in Theta, Alpha, and Gamma bands. Solid lines and segmented lines represent the holistic (HPS) and componential processing strategies (CPS), respectively. Mean phase-locking value (in standard deviation units) between all electrodes pairs and time are respectively indicated in the y and x axes of the graphs. Vertical lines indicate the onset of the fraction pairs. The rectangles delimit time windows showing significant differences between conditions. (B) Spatial distribution of phase synchrony for all pairs of electrodes. Black and red lines connect pairs of electrodes displaying significant synchronization and desynchronization, respectively ($p < 0.0000001$).

We performed the analysis of Power and PLV with Matlab 7.0.4 (Mathworks, Inc) using algorithms developed by Dr. Eugenio Rodriguez and others [12,14].

2.4.2. ERP

The continuous EEG signal was filtered off-line with a band-pass filter (0.5–30 Hz) type FIR Kaiser, which has a linear phase response. Then, the filtered signal was segmented into a series of 1200-ms-long epochs. Each epoch started 200 ms before the onset of a fraction pair and ended 1000 ms later. All epochs were corrected for eye blinks and eye movements [15,16]. Afterwards, trials containing voltage fluctuations that exceeded $\pm 200 \mu\text{V}$ or transients exceeding $\pm 100 \mu\text{V}$ were rejected. Artifact-free epochs were averaged in relation to the onset of the fractions pair, re-referenced off-line to the average activity of the mastoid electrodes [3] and baseline-corrected over a 200 ms window before the onset of the fraction pair. The EEGLAB Matlab toolbox was used for visualization [17].

2.5. Statistical analysis

2.5.1. Induced spectral power and phase synchrony

Because we were interested in long-range coordination of neural activity, our statistical analyses pool together all electrodes to produce a global index of synchronization across a large frequency range. The statistical analyses of the time-frequency and phase synchrony distributions were thus performed on time-frequency charts resulting from averaging the electrophysiological responses of all sensors during the entire segment (–1200 to 2400 ms after fraction pair onset). This resulted in a grand average time-frequency and a phase synchrony chart per experimental condition per subject. Then, those charts were grouped by condition and analyzed by means of a permutation test ($\alpha = 0.05$) in search of time-frequency windows showing significant effects. Subsequently, the significant time-frequency windows were analyzed with a within-subject ANOVA. The α level was set at 0.05 for all tests and, when necessary, we applied Greenhouse-Geisser correction.

For the topographical analysis of phase synchrony we controlled for the statistical effects of multiple comparisons by choosing a very conservative significance threshold ($p < 0.0000001$). This threshold was set on the basis of the distribution of synchrony values during the baseline. The threshold was chosen such that the number of

cases larger than the threshold divided by the total number of cases was equal to $p = 0.0000001$. By choosing this significance level, one line per analysis window could be explained by chance, given the fact that there were 59 electrodes with 1711 possible combinations ($59 \times 58/2 = 1711$) (for a similar method, see [8,18]).

2.5.2. ERP

In order to improve statistical power [19], electrodes were combined into four region of interest (left anterior: F1-F3-F5-F7-F17-FC1-FC3-FC5; right anterior: F2-F4-F6-F8-F18-FC2-FC4-FC6; left posterior: CP1-CP5-TP7-P1-P3-P5-P7-P9; right posterior: CP2-CP6-TP8-P2-P4-P6-P8-P10). Grand average ERPs grouped by condition were analyzed by means of a permutation test ($\alpha = 0.05$) in search of statistically significant differences between conditions. Subsequently, differences in mean amplitudes of the four region of interest between the two conditions were tested by repeated-measurement ANOVAs. The α level was set at 0.05 for all tests and, when necessary, we applied Greenhouse-Geisser correction.

3. Results

3.1. Behavioral

Percentage of correct answers in the CPS condition was 90.77% with an average response time of 783.16 ms, whereas in the HPS condition it was 85.81% with an average response time of 902.63 ms. Paired two tailed *t*-tests revealed that both accuracy ($t(14) = 3.21$, $p = .006$) and average response times ($t(14) = -2.62$, $p = .02$) were significantly different across conditions.

To confirm that participants engaged preferentially in componential processing for fraction pairs with common components and in holistic processing for fraction pairs without common components, we measured the relative contributions to performance of the numerical distance between fractions and fraction components. To do this, we used linear regressions on log-scaled response times for correctly answered trials, considering participants as a random factor. For a fraction pair a/b and c/d , its distance was measured as $\text{abs}(a/b - c/d)$, whereas the distance between fractions' components was quantified as $\text{abs}(a - c) + \text{abs}(b - d)$. Likelihood-ratio tests show that the distance between fraction components explains a significant share of variance only for trials with common components (with common components: $\chi^2(1) = 6.25$, $p = .01$;

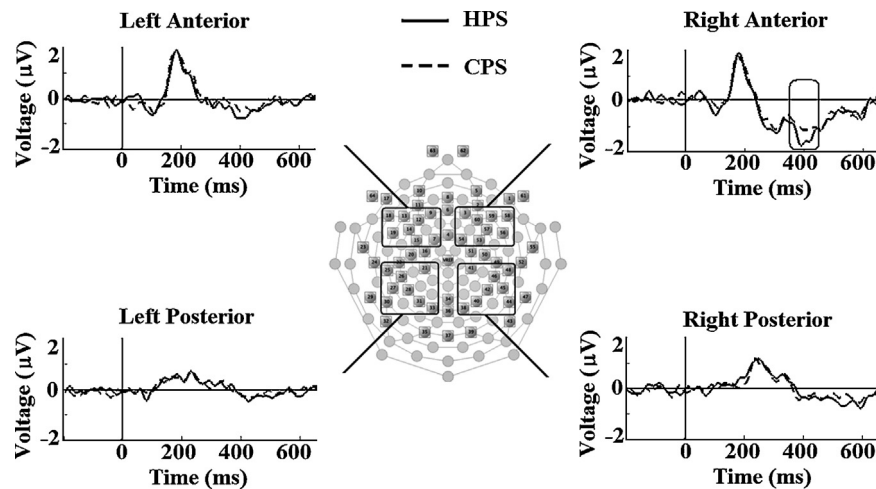


Fig. 2. Anterior negativity around 400 ms during fraction comparison task. Each graph shows the waveforms for the holistic (HPS: solid line) and componential (CPS: segmented line) processing strategies, for each one of the four ROIs (left anterior, left posterior, right anterior, and right posterior). Voltage (in microvolts) and time are respectively indicated in the y and x axes of the graphs. Vertical lines indicate the onset of the fraction pair. The rectangle indicates the ROI and time window that showed significant differences between conditions.

without: $X^2(1)=1.06$, $p=.30$), and that the distance between fractions significantly improves the fit only for trials without common components (with common components: $X^2(1)=1.00$, $p=.32$; without: $X^2(1)=24.7$, $p=.0000007$).

3.2. Phase synchrony

Results are shown in Fig. 1A. We found that mean Alpha phase synchrony (10–13 Hz) over all electrode pairs was significantly lower for the CPS than for the HPS from 300 ms to 400 ms after fraction pair onset (300–400 ms: $F(1,14)=5.108$, $p=.040$, $\eta^2=.267$). In addition, Theta phase synchrony was significantly higher for the HPS than for the CPS from 300ms to 500ms after fraction pair onset (Theta: 300–500 ms, $F(1,14)=9.170$, $p=.009$, $\eta^2=.396$). Similarly, Gamma phase synchrony was significantly higher for the HPS than for the CPS from 500 ms to 600 ms after fraction pair onset (Gamma: 500–600 ms: $F(1,14)=10.927$, $p=.005$, $\eta^2=.438$).

The spatial distribution of phase synchrony over the scalp for each experimental condition is depicted in Fig. 1B. In the case of the CPS, we found strong Alpha phase desynchronization among fronto-parietal sites mostly over the left side of the scalp, 300–400 ms after the onset of fraction pair. For the HPS, we observed an increase of Theta phase synchronization among bilateral frontal and parietal sites 300–500 ms after fraction pair onset, and an increase of Gamma phase synchronization among central-parietal and frontal sites 500–600 ms after fraction pair onset.

3.3. ERP

Results are shown in Fig. 2. Visual inspection of ERP waveforms shows three distinct components in frontal regions: P1 (20–70 ms), N1 (70–100 ms) and N4 (370–430 ms). We observed that the early P1 and N1 components do not differ significantly between conditions at either left frontal (P1: $F(1,14)=3.048$, $p=.103$; N1: $F(1,14)=0.972$, $p=.341$) or right frontal regions (P1: $F(1,14)=0.401$, $p=.537$; N1: $F(1,14)=1.201$, $p=.292$). In the case of the N4 component, we found that this late negative deflection of the ERP activity was significantly larger for the HPS than for the CPS over the right frontal region ($F(1,14)=5.817$, $p=.030$, $\eta^2=.294$).

Additionally, we computed bivariate correlations to investigate the relation between the mean amplitude of ERP negativity near 400 ms and the mean Theta, Alpha, and Gamma phase synchrony in both conditions. To homogenize both the reference

as the baseline of ERP and PLV for the correlation analysis, we used an average reference and baseline of 400 ms pre-stimulus for calculus of ERP. Given that normality tests (via normal P-P probability plots) indicated that ERP and PLV data were not normally distributed, Spearman's correlation coefficient (ρ) was used ($p < 0.05$). Calculation of Spearman's ρ revealed a significant correlation between the amplitude of right frontal negativity near 400 ms and Theta phase synchrony in both HPS and CPS conditions (HPS, $r_s(13)=-.582$, $p=.011$; CPS, $r_s(13)=-.450$, $p=.046$).

4. Discussion

The main goal of this study was to investigate the role played by neural synchronization when adults compare fractions with either a componential or holistic processing strategy. We found that local neural coupling did not differ between conditions, whereas large-scale synchronization patterns differed importantly. In what follows, we discuss these findings and their implications in detail.

Behavioral data indicate that the use of the CPS is associated with a higher accuracy rates and lower response times than the HPS. Both accuracy and response time can be interpreted as indices of task difficulty. In this sense, using the CPS for processing fractions would require less cognitive effort than the HPS, consistently with previous results [20]. However, it is important to note that due to the forced delay of subjects' responses, response times might not reflect faithfully the underlying neural processes.

Regarding the relation between EEG neuronal synchrony and fraction processing, that our results show, compared to the HPS, the CPS induces a strong Alpha phase desynchronization over left frontoparietal sites, regions traditionally associated with the representations of core number skills [21]. Alpha phase desynchronization has been proposed as a downregulation mechanism of cortical networks related to attention [22] and executive functions [23]. As for its role in the processing of fractions, we suggest that the connectivity restriction generated by Alpha neuronal decoupling would favor an efficient reallocation of cognitive resources in the global neuronal workspace [24]. Given a simple task that requires conscious control to be solved, such as comparing fractions with common components, the global neuronal workspace would be reorganized via Alpha desynchronization so that only those modules strictly necessary to solve the task stay connected. In contrast, a task that demands high cognitive effort, such as comparing fractions without common components, requires the coordination of

a larger number of processors in the global neuronal workspace. In this case, we observed an early increase of Theta phase synchrony over bilateral frontal and bilateral parietal cortical regions, and a late increase of Gamma phase synchrony over centroparietal and frontal regions. Numerous reports associate theta and gamma oscillations with working memory load [25] and perceptual binding [26], respectively. Moreover, both frequency bands have also been associated with encoding and retrieval of declarative memory [27]. Concerning the role played by neural coordination in these frequency bands during the fractions processing, we propose that early Theta phase synchrony signals the retention of numeric information in working memory, and late Gamma phase synchronization its subsequent integration. Alternatively, Theta and Gamma phase synchronization could be related with the increase of cognitive effort due to task difficulty.

In addition to the study of neural synchrony, the analysis of evoked activity revealed that early ERP components do not differ between conditions. These results depart from those of a previous study [3]. This could be explained by differences between the experimental paradigms used in both studies. Unlike the previous ERP study [3], we found that, compared to the CPS, the HPS evoked a negative deflection of the ERP around 400 ms post-stimulus. Traditionally, the negative amplitude of the ERP in this time window is considered an indicator of semantic processing [28]. Alternatively, it has been associated with various memory processes, such as recognition memory [29] and long-term memory retrieval [30], and also with interference effects in the numerical Stroop paradigm [31]. As for its role in the processing of fractions, we propose that the negative amplitude around 400 ms would be modulated by the degree of interference between the numerical value of the fraction components and the value of the fraction as a whole. Finally, the correlation between theta phase synchrony and the mean amplitude of ERP negativity near 400 ms may be interpreted as an indicator of the interplay between working memory load and the difficulty to access the magnitudes of the intervening fractions due to the interference generated by the numerical value of the components. Nevertheless, future experiments should directly address this issue.

In conclusion, the results of our study reveal how the brain dynamically self-organizes depending on the type of cognitive strategy used for comparing fractions with and without common components. Specifically, it seems that long-distance neural synchronization, and not local neural coupling, is involved in the use of different cognitive strategies for processing fractions, revealing the emergence of transient functional arithmetic networks widely distributed within the brain.

Acknowledgements

This research was supported by the Associative Research Program of CONICYT (CIE-05 and BASAL-CMM grants), and by the program CONICYT PAI/Academia (grant 79130005). We thank Eugenio Rodriguez for his comments.

References

- [1] G. Meert, J. Grégoire, M.P. Noël, Rational numbers: Componential vs. holistic representation of fractions in a magnitude comparison task, *Q. J. Exp. Psychol.* 62 (2009) 1598–1616.
- [2] M. Schneider, R.S. Siegler, Representations of the magnitudes of fractions, *J. Exp. Psychol. Hum. Percept. Perform.* 36 (2010) 1227–1238.
- [3] L. Zhang, Z. Xin, F. Li, Q. Wang, C. Ding, H. Li, An ERP study on the processing of common fractions, *Exp. Brain Res.* 217 (2012) 25–34.
- [4] A. Ischebeck, M. Schocke, M. Delazer, The processing and representation of fractions within the brain: An fMRI investigation, *Neuroimage* 47 (2009) 403–413.
- [5] S. Dehaene, L. Cohen, Towards an anatomical and functional model of number processing, *Math Cogn.* 1 (1995) 83–120.
- [6] F.J. Varela, J.P. Lachaux, E. Rodriguez, J. Martinerie, The brainweb: phase synchronization and large-scale integration, *Nat. Rev. Neurosci.* 2 (2001) 229–239.
- [7] N. Molinaro, P. Barraza, M. Carreiras, Long-range neural synchronization supports fast and efficient reading: EEG correlates of processing expected words in sentences, *Neuroimage* 72 (2013) 120–132.
- [8] A. Pérez, N. Molinaro, S. Mancini, P. Barraza, M. Carreiras, Oscillatory dynamics related to the unagreement pattern in Spanish, *Neuropsychologia* 50 (2012) 2584–2597.
- [9] E. Rodriguez, N. George, J.P. Lachaux, J. Martinerie, B. Renault, F. Varela, Perception's shadow: long-distance synchronization of human brain activity, *Nature* 397 (1999) 430–433.
- [10] C. Tallon-Baudry, O. Bertrand, Oscillatory gamma activity in humans and its role in object representation, *Trends Cogn. Sci.* 3 (1999) 151–162.
- [11] M. Bastiaansen, P. Hagoort, Oscillatory neuronal dynamics during language comprehension, *Prog. Brain Res.* 159 (2006) 179–196.
- [12] J.P. Lachaux, E. Rodríguez, J. Martinerie, F. Varela, Measuring phase synchrony in brain signals, *Hum. Brain Mapp.* 8 (1999) 194–208.
- [13] T.C. Ferree, P. Luu, G.S. Russell, D.M. Tucker, Scalp electrode impedance, infection risk, and EEG data quality, *Clin. Neurophysiol.* 112 (2001) 536–544.
- [14] M. Le Van Quyen, J. Foucher, J.P. Lachaux, E. Rodriguez, A. Lutz, J. Martinerie, F. Varela, Comparison of Hilbert transform and wavelet methods for the analysis of neuronal synchrony, *J. Neurosci. Meth.* 111 (2001) 83–98.
- [15] G. Gratton, M. Coles, E. Donchin, A new method for off-line removal of ocular artifacts, *Electroen. Clin. Neuro.* 55 (1983) 468–484.
- [16] G.A. Miller, G. Gratton, C.M. Yee, Generalized implementation of an eye movement correction procedure, *Psychophysiology* 25 (1988) 241–243.
- [17] A. Delorme, S. Makeig, EEGLAB: an open source toolbox for analysis of single-trial EEG dynamics including independent component analysis, *J. Neurosci. Meth.* 134 (2004) 9–21.
- [18] L. Melloni, C. Molina, M. Pena, D. Torres, W. Singer, E. Rodríguez, Synchronization of neural activity across cortical areas correlates with conscious perception, *J. Neurosci.* 27 (2007) 2858–2865.
- [19] B.S. Oken, K.H. Chiappa, Statistical issues concerning computerized analysis of brainwave topography, *Ann. Neurol.* 19 (1986) 493–497.
- [20] A. Obersteiner, W. Van Dooren, J. Van Hoof, L. Verschaffel, The natural number bias and magnitude representation in fraction comparison by expert mathematicians, *Learn Instr.* 28 (2013) 64–72.
- [21] S. Dehaene, N. Molko, L. Cohen, A.J. Wilson, Arithmetic and the brain, *Curr. Opin. Neurobiol.* 14 (2004) 218–224.
- [22] S. Sadaghiani, R. Scheeringa, K. Lehongre, B. Morillon, A.L. Giraud, M. D'Esposito, A. Kleinschmidt, Alpha-band phase synchrony is related to activity in the fronto-parietal adaptive control network, *J. Neurosci.* 32 (2012) 14305–14310.
- [23] S. Hanslmayr, G. Volberg, M. Wimber, N. Oehler, T. Staudigl, T. Hartmann, M. Raabe, M.W. Greenlee, K. Bäuml, Prefrontally driven down-regulation of neural synchrony mediates goal-directed forgetting, *J. Neurosci.* 32 (2012) 14742–14751.
- [24] S. Dehaene, M. Kerszberg, J.P. Changeux, A neuronal model of a global workspace in effortful cognitive tasks, *PNAS* 95 (1998) 14529–14534.
- [25] J. Fell, N. Axmacher, The role of phase synchronization in memory processes, *Nat. Rev. Neurosci.* 12 (2011) 105–118.
- [26] A.K. Engel, P. Fries, W. Singer, Dynamic predictions: oscillations and synchrony in top-down processing, *Nat. Rev. Neurosci.* 2 (2001) 704–716.
- [27] D. Osipova, A. Takashima, R. Oostenveld, G. Fernández, E. Maris, O. Jensen, Theta and gamma oscillations predict encoding and retrieval of declarative memory, *J. Neurosci.* 26 (2006) 7523–7531.
- [28] M. Kutas, S. Hillyard, Event-related brain potentials to semantically inappropriate and surprisingly large words, *Biol. Psychol.* 11 (1980) 99–116.
- [29] M. Rugg, T. Curran, Event-related potentials and recognition memory, *Trends Cogn. Sci.* 11 (2007) 251–257.
- [30] M. Niedeggen, F. Rösler, N400 effects reflect activation spread during retrieval of arithmetic facts, *Psychol. Sci.* 10 (1999) 271–276.
- [31] D. Szűcs, F. Soltész, Event-related potentials dissociate facilitation and interference effects in the numerical Stroop paradigm, *Neuropsychologia* 45 (2007) 3190–3202.